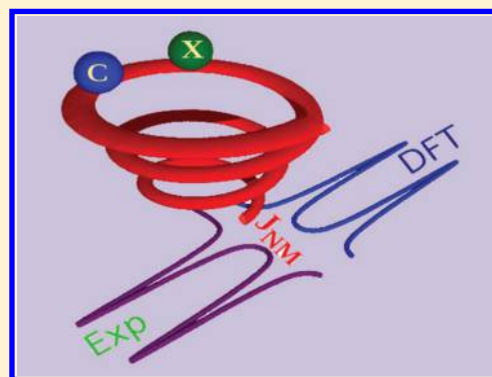


Improvements in DFT Calculations of Spin–Spin Coupling Constants

J. San Fabián,[†] J. M. García de la Vega,^{*,†} and E. San Fabián[‡][†]Departamento de Química Física Aplicada, Facultad de Ciencias, Universidad Autónoma de Madrid, 28049 Madrid, Spain[‡]Departamento de Química Física, Unidad Asociada del CSIC and Instituto Universitario de Materiales, Universidad de Alicante, San Vicente del Raspeig, 03690 Alicante, Spain

S Supporting Information

ABSTRACT: Different types of spin–spin coupling constants (SSCCs) for several representative small molecules are evaluated and analyzed using a combination of 10 exchange functionals with 12 correlation functionals. For comparison, calculations performed using MCSCF, SOPPA, other common DFT methods, and also experimental data are considered. A detailed study of the percentage of Hartree–Fock exchange energy in SSCCs and in its four contributions is carried out. From the above analysis, a combined functional formed with local Slater (34%), Hartree–Fock exchange (66%), and P86 correlation functional (S66P86) is proposed in this paper. The accuracy of the values obtained with this hybrid functional (mean absolute deviation of 4.5 Hz) is similar to that of the SOPPA method (mean absolute deviation of 4.6 Hz).



1. INTRODUCTION

The indirect nuclear spin–spin coupling constant (SSCC) is one of the most important parameters derived from nuclear magnetic resonance spectra. The relevance of this parameter lies in its close relationship with the electronic structure and therefore with the molecular structure. Calculated SSCCs can be formulated within the Ramsey nonrelativistic theory as originating from four different terms, Fermi contact (FC), spin–dipole (SD), paramagnetic spin–orbit (PSO), and diamagnetic spin–orbit (DSO):

$$^nJ_{NM} = ^nJ_{NM}^{FC} + ^nJ_{NM}^{SD} + ^nJ_{NM}^{PSO} + ^nJ_{NM}^{DSO} \quad (1)$$

where n denotes the number of chemical bonds between coupled nuclei N and M . The FC contribution is the largest contribution for several types of SSCCs. However, the remaining terms are also important when the coupling pathway involves either multiple bonds or nuclei with lone pair electrons. At present, density functional theory (DFT) is the most popular method to compute electronic structure and properties of molecules,¹ and since the pioneering work by Malkin et al.,² it has been successfully applied to the prediction of SSCCs,^{3–5} showing the best compromise between accuracy and computational cost. However, as stated by Helgaker,⁴ referring to Bartlett et al.:⁶ “although DFT has a rigorous base, in application is semi-empirical and there is no way to systematically to converge to the exact result”.

Some authors have shown that the most used functional, the hybrid B3LYP,^{7,8} is a good option to predict accurate SSCCs.^{9–14} However, our studies of $^1J_{CC}$ and $^1J_{CH}$ SSCCs^{5,15} suggest that this functional overestimates the calculated values. This overestimation can be ameliorated using relatively small basis sets as TZVP.^{16,17} Several other density functionals have been used to predict SSCCs. The generalized gradient approximated (GGA) functional PBE^{18,19} seems to yield the best results over

other 20 functionals and even to outperform B3LYP for the prediction of $^1J_{CH}$.²⁰ Cunha Neto et al.²¹ obtained reliable results using PBE^{18,19} for calculating $^1J_{CH}$ in 2-substituted tetrahydropyrans. PW91,^{22–24} B3P86,^{7,25} B97-2,²⁶ and the above-mentioned PBE were the GGA and the hybrid functional that performed best in Maximoff et al. study.²⁰ Hybrid B97-2 has also been suggested by Keal et al.²⁷ for the calculation of $^1J_{CH}$ in combination with aug-cc-pVTZ-J²⁸ basis set. Recently, Kupka et al.²⁹ tested the performance of 43 functionals to predict SSCCs in small molecules. They found good performance using the B97 family functionals for $^1J_{CC}$, $^yJ_{XH}$ ($y = 1, 2$, and 3) and $^xJ_{HH}$ ($x = 1, 2$).

The effect of changing the amount of exact Hartree–Fock (HF) exchange and electronic correlation in the calculation of SSCCs has previously been investigated.^{9,10,29} Cremer et al.,⁹ in the same work where the coupled perturbed density functional theory (CPDFT) was implemented to calculate SSCCs, made an analysis of the SSCCs dependence on the exchange correlation (XC) functional and on the exact exchange. They carried out calculations using different XC energy

$$E_{XC}(a_x) = (1 - a_x)(E_X^B + E_C^{LYP}) + a_x E_X^{HF} \quad (2)$$

where E_X^B , E_C^{LYP} , and E_X^{HF} are, respectively, Becke exchange energy, LYP correlation energy and HF exchange energy and with $a_x = 0.0, 0.1, 0.5, 0.9$, and 1.0 . Results with $a_x = 0.0$ and $a_x = 1.0$ correspond to the true BLYP functional and HF, respectively. For the set of SSCCs studied in that work, they proposed to use the B3LYP functional because it yields the lower mean absolute deviation (mad). It should be noted that applying the strategy proposed in this paper to the data set of Cremer et al.,⁹ the mad

Received: July 28, 2014

obtained with B3LYP (5.0 r.u.) is predicted to drop to 4.0 r.u. using the BLYP with $a_x = 0.29$. Helgaker et al.¹⁰ analyzed the results obtained with B3LYP changing the amount of exact HF exchange to 15%, 20% (true B3LYP), and 25%. They concluded that the SSCCs cannot be improved simply by adjusting the HF exchange. Kupka et al.²⁹ also studied the effect of correlation, long-range-correlation, and exact exchange on calculated SSCCs. Their main remarks are that P86 correlation functional is better than LYP and PW91 for calculating SSCCs; the long-range-corrected CAM-B3LYP improves 1J values, but worsens slightly those of 2J and 3J . Moreover, the effect of considering a percentage of the exact exchange functional is very dependent on the SSCC type. Nevertheless, they found²⁹ that an amount between 20 and 50% is a good compromise for SSCCs.

Since the early 1990s, the standard hybrid functionals^{7,30} have proved to give good performance for predicting various molecular properties.³¹ Hybrid functionals include a portion of exact HF exchange and evaluate the remainder exchange from the base functional used. In the HF method, the exact exchange cancels out the self-Coulomb energy, and therefore, the incorporation of a fraction of this exact-exchange will ameliorate the wrong asymptotic behavior attributed to DFT^{32–35} while retaining a reasonable simulation of dynamical and non-dynamical correlation. The hybrid functionals only deal with the inclusion of Fock exchange, whereas correlation effects are described with the traditional approach of DFT. Global hybrid functionals, which include a constant exact exchange admixture, have been recently extended, in the so-called local hybrid functionals, to consider position-dependent admixture of DFT exchange and exact exchange.³⁶ It has been shown that the use of global or local hybrid functionals can be successful.^{36–38}

In this study, we try to find out a way to improve hybrid functionals in order to calculate different types of SSCCs in different molecules. This work presents two main targets: first, to study how SSCCs behave when they are calculated using different combinations of exchange-correlation functionals and second, using the previously obtained results, to propose a simple hybrid functional whose potential exchange will consist of a combination of the Slater^{39,40} and Hartree–Fock exchange, to obtain the best values of different kinds of SSCCs.

The paper is organized as follows: Computational Details section describes the DFT calculations carried out for the selected constants and molecules. Next the analysis of calculated FC, SD, PSO, and DSO contributions for one, two, and three bond SSCCs is carried out (section 3). The variation of these contributions with the proportion of Slater and HF exchange is discussed (section 4). The great dependence of the SSCCs on the exact HF exchange functional makes us to propose three possible optimization models. Results obtained for the studied SSCC data set with these proposed hybrid functionals are discussed (section 5). At the end, some concluding remarks are gathered.

2. COMPUTATIONAL DETAILS

One-, two-, and three-bond SSCCs between different first row nuclei (H, O, N, C, and F) have been calculated for representative small molecules (CH_4 , C_2H_6 , C_2H_4 , C_2H_2 , HCN , CH_3F , C_3H_4 , H_2 , NH_3 , H_2O , HF , CO , CO_2 , and N_2). All SSCCs (45 values) for those molecules have been considered, and the four contributions (FC, SD, PSO, and DSO) have been calculated. Experimental geometries were used.⁴¹ The choice of these molecules/SSCCs is due to the following features: (i) wide variety of nuclei involved in the couplings, (ii) couplings through different types of bonds (single, double, triple), and (iii) this data

set has been analyzed in detail using the MCSCF and SOPPA methods.⁴¹ Hence, our results of the calculated total SSCCs can be compared with experimental values and also with the different contributions (FC, SD, ...), experimentally unobtainable.

Two main groups of functionals have been used in this work. First, the large group corresponds to the combination of 10 exchange functionals: B88,⁴² PW91,^{22–24} G96,^{43,44} PBE,^{18,19} mPW,⁴⁵ PBEh,⁴⁶ OPTX,^{47,48} BRx,⁴⁹ PKZB,⁵⁰ and TPSS⁵¹ with 12 correlation ones: VWN,⁵² VWN5,⁵² PL (Perdew Local in the nomenclature of Gaussian package, also known as PZ81),⁵³ P86,²⁵ VP86 (combination of VWN5 local and P86 nonlocal),⁵⁴ PW91,^{22–24} PBE,^{18,19} B95,⁵⁵ LYP,⁸ KCIS,^{56–58} PKZB,⁵⁰ and TPSS.⁵¹ Also results obtained only with the exchange functional (denoted as No-corr) are included in this group. The reason for choosing these functionals is purely systematic. We try to scan all the density functionals implemented in the Gaussian program⁵⁴ that allow the independent combination of exchange and correlation functionals. These functionals include local density approximations, generalized gradient approximations (GGA), and meta-GGAs. Recently, many efforts have been conducted to the development of functionals to give good description of weak interactions like dispersion and van der Waals interactions. However, these functionals do not seem to be important for SSCCs, specially for the FC contribution where the correct description of the wave function close to the nuclei is essential. The second group of functionals are those formed with local Slater⁵⁹ and a percentage of exact HF exchange in combination with LYP,⁸ P86,²⁵ or VWN5⁵² correlation functionals as well as with no correlation functional. They will be denoted as SmmCOR, where S indicates the Slater exchange functional, mm is a two-digit number that shows the percentage of HF exchange, and COR is the used correlation functional (LYP, P86, VWN5, or none).

MCSCF, SOPPA, and SOPPA(CCSD)^{60–62} wave function methods and some common hybrid functionals were used for comparison purposes. All calculations were carried out with the aug-cc-pVTZ-J basis set.²⁸ This basis set was specially built for SSCCs and yields values close to those obtained within the complete basis set limit approach.^{29,63} In combination with the B3LYP functional, this basis set was proposed as an excellent alternative for calculating SSCC in large molecules.⁶³ Recently, we have shown for a large data set of $^1J_{\text{CH}}$ SSCCs that using basis sets larger than aug-cc-pVTZ-J, namely, ccJ-pVQZ⁶⁴ and pcJ-3,⁶⁵ combined with popular functionals does not yield a significant improvement.¹⁵ The Gaussian suite of programs⁵⁴ was used in all the calculations. The experimental (39 out of 45 calculated) values used in the present work as reference correspond to those obtained after subtracting the vibrational corrections.⁴¹

Besides the SSCC $^nJ_{\text{NM}}$ in frequency units, which are appropriated from an experimental point of view, we will use reduced spin–spin coupling constant $^nK_{\text{NM}}$ (RSSCC), which only reflects the electronic coupling mechanism between the nuclei. Experimental SSCC $^nJ_{\text{NM}}$ depends on the magnetogiric ratios γ_{N} and γ_{M} of the two coupling nuclei

$$^nJ_{\text{NM}} = h \frac{\gamma_{\text{N}}\gamma_{\text{M}}}{4\pi^2} ^nK_{\text{NM}} \quad (3)$$

The use of RSSCC removes the isotope dependence and allows an analysis of different effects based on electronic mechanisms that for this multinuclear study is more appropriate. For these RSSCCs, reduced units (r.u.) of $10^{19}\text{T}^2\text{J}^{-1}$ will be used.⁴¹ The RSSCC can be split in the four Ramsey contributions

$$^nK_{\text{NM}} = ^nK_{\text{NM}}^{\text{FC}} + ^nK_{\text{NM}}^{\text{SD}} + ^nK_{\text{NM}}^{\text{PSO}} + ^nK_{\text{NM}}^{\text{DSO}} \quad (4)$$

3. ANALYSIS OF CONTRIBUTIONS TO SSCCS

First, we review briefly the definition and evaluation of SSCCs.^{4,9,10} ${}^nK_{NM}$ RSSCCs are given as the second derivatives of the total ground state energy E with respect to the nuclear magnetic moments μ as follows:

$${}^nK_{NM} = \frac{d^2E}{d\mu_N d\mu_M} \bigg|_{\mu=0} \quad (5)$$

Only the isotropic value $(1/3)\text{Tr}[K_{NM}]$ contributes to the measurement spectrum of orientationally averaged molecules. In CPDFT,⁹ the isotropic RSSCC can be decomposed into the sum of four Ramsey coupling mechanisms represented as

$${}^nK_{NM} = \frac{2}{3} \sum_{i\sigma} \langle \psi_{i\sigma}^{(0)} | h_N^{FC} | \psi_{i\sigma}^{(M)FC} \rangle + \frac{2}{3} \sum_{i\sigma} \langle \psi_{i\sigma}^{(0)} | h_N^{SD} | \psi_{i\sigma}^{(M)SD} \rangle \quad (6)$$

$$- \frac{4}{3} \sum_i \langle \phi_i^{(0)} | h_N^{PSO} | \phi_i^{(M)PSO} \rangle + \frac{2}{3} \sum_i \langle \phi_i^{(0)} | \text{Tr} h_{NM}^{DSO} | \phi_i^{(0)} \rangle \quad (7)$$

where FC and SD contributions are expressed in terms of spin-dependent orbital $\psi_{i\sigma}$ while PSO and DSO are written in terms of spin-free orbitals ϕ_i . Zeroth-order orbitals are denoted by superscript (0), whereas superscript (M) denotes first-order orbitals resulting from the perturbation at nucleus M. The index i denotes occupied orbitals, while σ is the spin variable. h_N^{FC} , h_N^{SD} , h_N^{PSO} , and h_N^{DSO} are one-particle operators that are expressed in atomic units as

$$h_N^{FC} = \frac{8\pi\alpha^2}{3} \delta(\mathbf{r}_N) \mathbf{s} \quad (8)$$

$$h_N^{SD} = \alpha^2 \left(3 \frac{(\mathbf{s} \cdot \mathbf{r}_N) \mathbf{r}_N}{r_N^5} - \frac{\mathbf{s}}{r_N^3} \right) \quad (9)$$

$$h_N^{PSO} = \alpha^2 \frac{\mathbf{r}_N}{r_N^3} \times \nabla \quad (10)$$

$$h_N^{DSO} = \alpha^4 \left(\frac{\mathbf{r}_N}{r_N^3} \frac{\mathbf{r}_M}{r_M^3} \mathbf{1} - \frac{\mathbf{r}_N}{r_N^3} \circ \frac{\mathbf{r}_M}{r_M^3} \right) \quad (11)$$

α is the fine-structure constant, $\delta(\mathbf{r}_N)$ is the Dirac delta function, \mathbf{r}_N is the electron position with respect to the magnetic nucleus N, \mathbf{s} is the electron spin, and $\mathbf{1}$ is the unitary vector.

In order to analyze the effects of the different exchange and correlation functionals for the four different contributions (FC, SD, PSO, and DSO) the computed RSSCCs are summarized in Figure S1 (Supporting Information). In these representations, results previously calculated at the MCSCF,⁴¹ those obtained with the Slater functional and those calculated at the HF are also shown (horizontal lines) for comparison purposes. In Table 1, the largest variations of the FC, SD, and PSO contributions with the exchange and with the correlation functional are collected. To determine them, we consider any correlation functional (or any exchange functional), then the maximum deviation between two exchange functionals (or between two correlation functionals) is obtained. Table 1 gives a rough idea about the variation of the different contributions with the exchange or correlation functional and their relative importance. This table presents the results for the reduced contributions in r.u., a similar table for frequency units (Hz) is included in the Supporting Information (Table S1). The variations for DSO contributions

Table 1. Maximum Exchange Functional Variations (MXFV) and Maximum Correlation Functional Variations (MCFV) of Reduced Constants^a (r.u.) for FC, SD, and PSO Contributions^b

molecule	RSSCC	FC		SD		PSO	
		MXFV	MCFV	MXFV	MCFV	MXFV	MCFV
CH ₄	¹ K _{CH}	10.7	8.2	—	—	0.1	—
C ₂ H ₆	¹ K _{CH}	10.4	8.2	—	—	0.1	—
C ₂ H ₄	¹ K _{CH}	11.8	9.8	—	—	—	—
C ₂ H ₂	¹ K _{CH}	16.0	14.8	0.1	0.1	0.1	—
HCN	¹ K _{CH}	18.6	15.3	0.1	0.1	0.1	—
CH ₃ F	¹ K _{CH}	12.0	9.3	0.1	—	—	—
C ₃ H ₄	¹ K _{C₃H₃}	11.8	9.3	—	—	0.1	—
C ₃ H ₄	¹ K _{C₁H₁}	15.3	12.0	—	—	0.1	—
C ₂ H ₆	¹ K _{CC}	17.4	20.4	0.3	0.2	0.1	0.1
C ₂ H ₄	¹ K _{CC}	24.0	28.8	1.3	3.1	1.6	0.5
C ₂ H ₂	¹ K _{CC}	30.5	34.2	2.6	5.4	1.2	0.9
C ₃ H ₄	¹ K _{C₁C₃}	8.5	11.6	0.2	0.2	0.1	0.1
C ₃ H ₄	¹ K _{C₁C₂}	23.9	25.9	1.4	3.5	1.0	0.3
H ₂	¹ K _{HH}	6.5	13.2	0.1	0.1	0.1	—
NH ₃	¹ K _{NH}	13.2	7.9	0.1	0.1	0.2	0.1
H ₂ O	¹ K _{HO}	15.3	5.6	0.1	0.1	0.6	0.1
HF	¹ K _{HF}	21.1	4.7	0.2	0.2	1.5	0.4
CO	¹ K _{CO}	16.2	13.9	1.6	3.4	3.4	2.1
CO ₂	¹ K _{CO}	27.1	11.8	0.7	1.1	1.1	0.3
HCN	¹ K _{CN}	32.2	23.7	3.9	7.4	0.6	0.9
N ₂	¹ K _{NN}	20.3	16.3	5.0	8.5	3.2	2.3
CH ₃ F	¹ K _{FC}	6.3	8.5	0.9	0.3	1.9	1.6
CH ₄	² K _{HH}	0.5	0.7	—	—	—	—
NH ₃	² K _{HH}	0.4	0.6	—	—	—	—
H ₂ O	² K _{HH}	0.5	0.5	—	—	—	—
C ₂ H ₆	² K _{HH}	0.5	0.7	—	—	—	—
C ₂ H ₄	² K _{HH}	0.6	0.6	—	—	—	—
CH ₃ F	² K _{HH}	0.6	0.7	—	—	—	—
C ₃ H ₄	² K _{H₃H₃'}	0.5	0.5	—	—	—	—
C ₂ H ₆	² K _{CH}	0.8	1.3	—	—	—	—
C ₂ H ₄	² K _{CH}	1.8	2.8	—	—	—	—
C ₂ H ₂	² K _{CH}	2.1	2.4	0.1	0.1	0.1	0.1
C ₃ H ₄	² K _{C₃H₁}	0.7	0.6	—	—	—	—
C ₃ H ₄	² K _{C₁H₃}	0.5	0.9	—	—	—	—
C ₃ H ₄	² K _{C₁H₂}	1.4	3.0	—	—	—	—
HCN	² K _{NH}	1.6	1.4	0.1	0.2	0.2	0.1
CO ₂	² K _{OO}	5.0	2.5	3.5	2.9	4.0	1.5
CH ₃ F	² K _{HF}	1.4	0.9	—	—	0.1	0.1
C ₂ H ₆	³ K _{HHg}	0.1	0.1	—	—	—	—
C ₂ H ₆	³ K _{HHt}	0.4	0.3	—	—	—	—
C ₂ H ₄	³ K _{HHc}	0.3	0.4	—	—	—	—
C ₂ H ₄	³ K _{HHt}	0.4	0.5	—	—	—	—
C ₂ H ₂	³ K _{HH}	0.4	0.7	—	—	—	—
C ₃ H ₄	³ K _{H₁H₃}	0.1	0.1	—	—	—	—
C ₃ H ₄	³ K _{H₁H₂}	0.2	0.3	—	—	—	—

^aSee Supporting Information for Hz units. ^bFor the DSO contribution, the maximum effects are smaller than 0.1 r.u. Values not shown are smaller than 0.05 r.u.

are not included in these tables owing to their small values (<0.1 r.u. or Hz).

Figure 1 presents a small selection of those results for the FC contributions shown in Figure S1. The three upper graphics in Figure 1 represent one-, two-, and three-bond RSSCCs showing

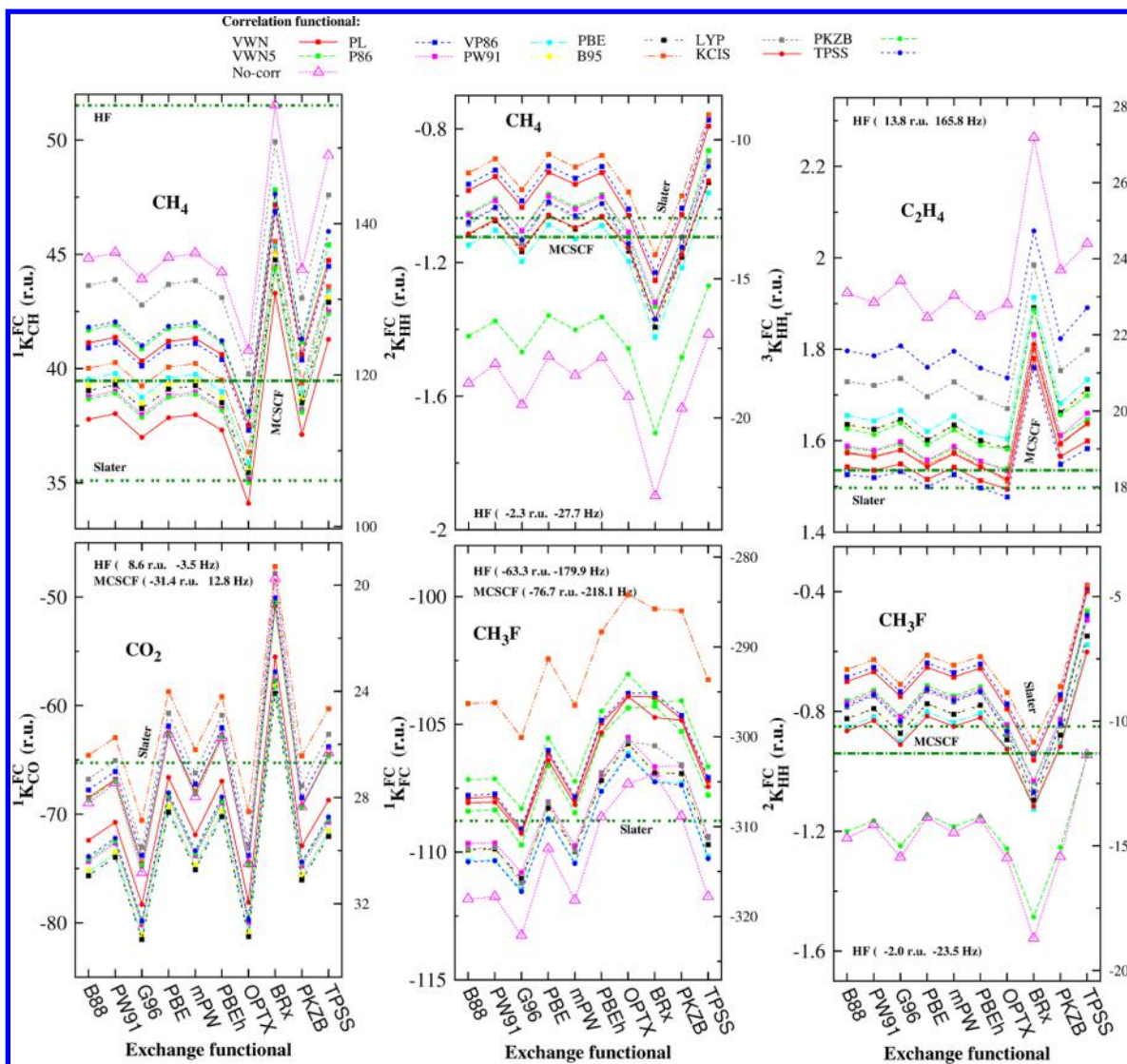


Figure 1. ${}^nK_{NM}^{FC}$ contributions calculated with different exchange (horizontal axis) and correlation (different curves) functionals for the indicated molecules. Right-hand scale corresponds to ${}^nJ_{NM}^{FC}$ in Hz units.

the general behavior discussed below, while the three lower ones correspond to values that deviate from that general behavior. All calculated ${}^1K_{NM}^{FC}$ contributions follow the same pattern

$${}^1K_{NM}^{FC}(HF) > {}^1K_{NM}^{FC}(MCSCF) > {}^1K_{NM}^{FC}(Slater) \quad (12)$$

The OPTX and G96 exchange functionals yield small ${}^1K_{NM}^{FC}$ values while BRx and TPSS exchange functionals give the largest ones. The BRx functional⁴⁹ yields results that tend to the HF values. It should be noted that this functional was designed⁴⁹ to reproduce the exact exchange energy of any 1s hydrogenic atom and to generate exchange energies in good agreement with the exact HF results in atomic systems.⁴⁹ Results from the remaining exchange functionals are roughly equivalent, showing small differences among them. Correlation functionals decrease the magnitude of ${}^1K_{NM}^{FC}$ contributions, distancing them from the MCSCF values. Results obtained without correlation functional (No-corr or pink triangles curves) are above the others for positive values and below for negative ones (Figure S1). The only two exceptions to this behavior are ${}^1K_{FC}^{FC}(\text{CH}_3\text{F})$ and ${}^1K_{CO}^{FC}$ (CO_2). The LYP correlation functional yields values (gray squares in Figure 1) close to those obtained without correlation.

Therefore, the correlation effect of this functional on ${}^1K_{NM}^{FC}$ is small compared with that of the other correlation functionals. For ${}^1K_{CH}^{FC}$ and ${}^1K_{CC}^{FC}$ the KCIS correlation functional yields the largest effects, that is, the largest reduction in the contributions. Considering the variation of FC with the exchange and correlation functionals (Table 1), we noted that the largest variations (in r.u.) correspond to ${}^1K_{NM}^{FC}$ through a double or triple bond. Thus, the two most important are those of ${}^1K_{CN}^{FC}$ (HCN) and ${}^1K_{CC}^{FC}$ (C_2H_2) that amount 32.3/23.7 r.u. and 30.5/34.2 r.u. for exchange/correlation functional, respectively (see Table 1). In Hz units, one of the largest variations (Table S1) is that of ${}^1K_{FH}^{FC}$ (HF molecule) amounting 239 Hz (21.1 r.u.) / 53 Hz (4.7 r.u.) for the exchange/correlation functionals. The variation of 239 Hz comes from the large values obtained with the BRx exchange functional with regard to the remaining ones. It is worth to note that the results of BRx exchange functional are closer to those of the MCSCF (see Figure S1 in the Supporting Information).

For two bond ${}^2K_{NM}^{FC}$ contributions, MCSCF results fall between those of Slater and HF with three exceptions (see Figure 2). These are ${}^2K_{H_3H_3}^{FC}$ in cyclopropane, ${}^2K_{CH}^{FC}$ in acetylene and ${}^2K_{NH}^{FC}$ in

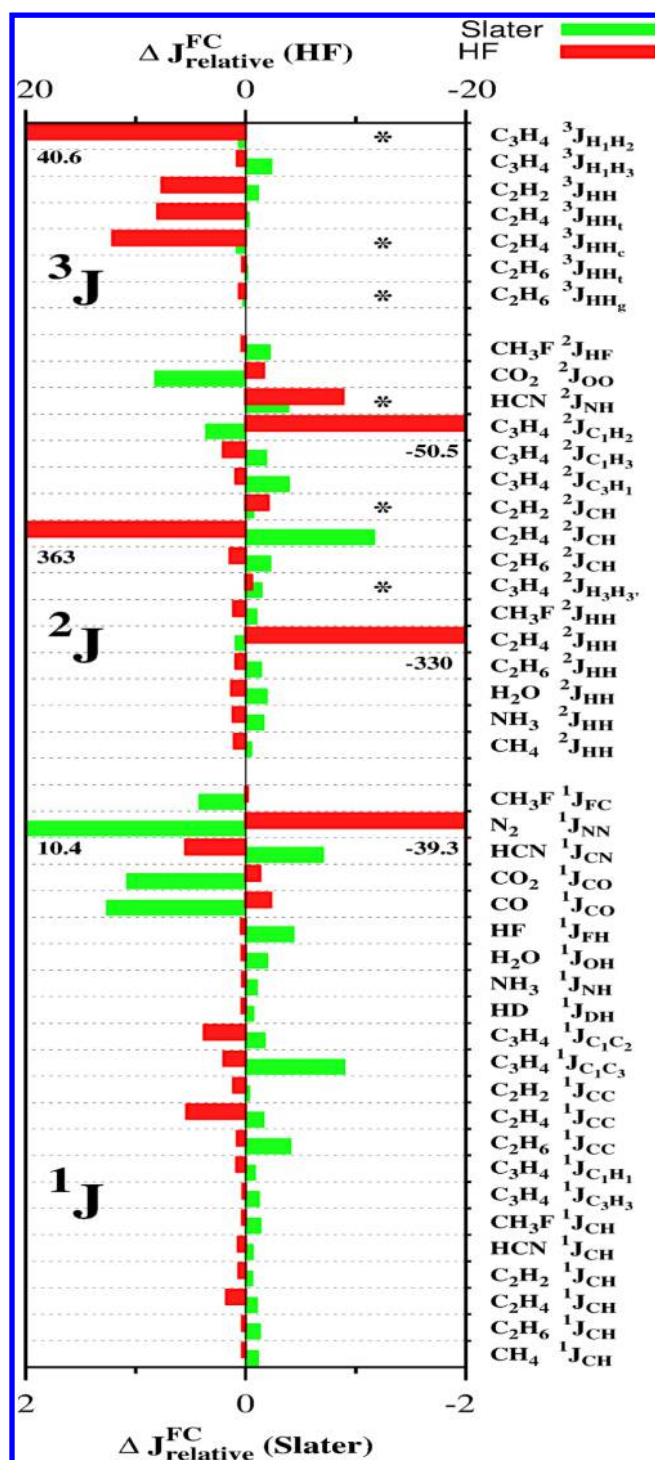


Figure 2. FC relative deviations $[J^{\text{FC}}(\text{Slater or HF}) - J^{\text{FC}}(\text{MCSCF})]/J^{\text{FC}}(\text{MCSCF})$. Out of range values are indicated numerically, and the SSCs where the MCSCF results are not among those of Slater and HF are shown with an asterisk. Notice the different scale used for Slater and HF.

hydrogen cyanide. In a fourth contribution, that of ${}^2K_{\text{HH}}^{\text{FC}}$ in ethylene, the MCSCF and Slater values are similar (0.04 r.u.). In general, ${}^2K_{\text{NM}}^{\text{FC}}$ presents negative values and then from highest to lowest we obtained Slater, MCSCF, and HF. In only one case, ${}^2K_{\text{HF}}^{\text{FC}}$ in CH_3F , the calculated values are positive and the indicated relation is reversed. Maximum and minimum values, which depend on the specific SSCs, are obtained using BRx,

OPTX, and TPSS exchange functionals. In most of the couplings, it is remarkable that the large deviation of the BRx exchange functional results with respect to the others. The correlation functional affects the ${}^2K_{\text{NM}}^{\text{FC}}$ contribution, increasing their values. Curve No-corr (pink triangles) falls always below (see Figure 1), except ${}^2K_{\text{HF}}^{\text{FC}}(\text{CH}_3\text{F})$ that yields the reverse behavior. It is worth noting that occasionally the results obtained with the meta-GGA PKZB correlation functional are close to those obtained without correlation (No-corr). The variations with the exchange/correlation functionals are smaller than those of ${}^1K_{\text{NM}}^{\text{FC}}$ amounting between 0.4 and 5 r.u. This last figure corresponds to ${}^2K_{\text{OO}}^{\text{FC}}$ in CO_2 (Table 1).

For three bond FC contributions, again, the behavior is similar to that shown above, that is, the MCSCF results fall between those of Slater and HF. The exceptions are ${}^3K_{\text{HH}_2}^{\text{FC}}$ (ethane), ${}^3K_{\text{HH}_1}^{\text{FC}}$ (ethene), and ${}^3K_{\text{H}_1\text{H}_2}^{\text{FC}}$ (cyclopropene) where MCSCF and Slater results are close. BRx exchange functional yields the largest values in magnitude, and the correlation functionals reduce that magnitude. The curve No-corr is above the remaining ones except that of ${}^3K_{\text{H}_1\text{H}_3}^{\text{FC}}$ (cyclopropene), the only one that presents negative values.

For SD contributions, the following general trends are observed from Figure S1: (i) SD values are smaller and change much less with the chosen functional than those of FC (see Table 1). Only ${}^1K_{\text{NN}}$ in N_2 and ${}^2K_{\text{CO}}$ in CO_2 present larger SD than FC contributions in magnitude. In the first case, the FC contribution is very small (−2.3 r.u), whereas the SD and PSO amount to 21.1 and −33.3 r.u., respectively, according to the MCSCF results.⁴¹ For the CO_2 coupling, the SD contributions is one of the most important (24.0 r.u.). Unfortunately, the experimental value for this geminal coupling is not obtainable. Regarding the variation of this contribution with the exchange functional (see Table 1), the three major changes lie between 3.5 and 5.0 r.u. in ${}^2K_{\text{CO}}^{\text{SD}}(\text{CO}_2)$, ${}^1J_{\text{CN}}^{\text{SD}}(\text{HCN})$, and ${}^1J_{\text{NN}}^{\text{SD}}(\text{N}_2)$. With regard to the correlation functional, variations larger than 3.5 r.u. correspond to ${}^1J_{\text{C}_1\text{C}_2}^{\text{SD}}$ in C_3H_4 (3.5 r.u.), ${}^1J_{\text{CC}}^{\text{SD}}$ in C_2H_2 (5.4 r.u.), ${}^1J_{\text{CN}}^{\text{SD}}$ in HCN (7.4 r.u.), and ${}^1J_{\text{NN}}^{\text{SD}}$ in N_2 (8.5 r.u.). The variations of both exchange and correlation functionals are of same order (Table 1). The correlation functional effect on the SD contribution is qualitatively independent of the used exchange functional. (ii) SD contributions calculated with the OPTX, BRx, PKZB, and TPSS exchange functionals present often the largest deviations on the average values. (iii) Correlation functional decreases the SD values, that is, the No-corr curve (pink triangles) is above the remaining ones (Figure S1). This agrees with the results obtained previously⁴¹ at MCSCF level where the effects of tri-, tetra- and polielectronic excitations, the increase of electronic correlation, tend to decrease the SD contributions. (iv) B95 and, in a minor amount, KCIS correlation functionals yield the smaller values, opposite to the No-corr values, that is, they include the largest correlation effect on the SD contribution. (v) Usually, the local Slater exchange functional yields results close to those of the MCSCF. The SD MCSCF results for the set of 45 calculated values are reproduced using the Slater functional with a root-mean-square deviation/mean absolute deviation (rmsd/mad) of 0.28/0.14 r.u. (0.92/0.27 Hz). These values include the large deviation shown by ${}^1J_{\text{FH}}^{\text{SD}}(\text{HF molecule})$ that is 6 Hz, which is the only one greater than 1 Hz. Ignoring the HF molecule, the resulting rmsd/mad is 0.21/0.14 Hz. This suggests that this contribution can be calculated using this inexpensive local functional.

Exceptions to this general behavior are found mainly when a coupled fluorine is involved. Thus, in ${}^1K_{\text{HF}}^{\text{SD}}(\text{HF})$ the correlation

functional B95 yields results close to those obtained without correlation (No-corr curve). In addition, for ${}^1K_{FC}^{SD}(\text{CH}_3\text{F})$, ${}^2K_{CH}^{SD}(\text{C}_2\text{H}_2)$, and ${}^2K_{HF}^{SD}(\text{CH}_3\text{F})$, the correlation functional increases the SD contributions instead of decreasing it. It should be noted that the HF molecule has been frequently omitted from statistical analysis owing to its challenging behavior.^{2,10,27,66}

The behavior of the PSO contribution is less uniform than that of the SD one (see Figure S1 and Table 1). Nevertheless, the following general trends can be observed. For some RSSCCs, the relative importance of PSO contribution is higher than that of the SD. However, its variation with the exchange or correlation functional is of the same order or slightly smaller (Table 1). Thus, for the largest values, ${}^1K_{NN}^{PSO}(\text{N}_2)$ and ${}^1K_{CO}^{PSO}(\text{CO})$ that amount -33.3 and -32.1 r.u.,⁴¹ respectively, the maximum change with the exchange or correlation functional is 3.4 r.u. (roughly 10%). The largest value in Hz corresponds to ${}^1J_{HF}^{PSO}(\text{HF})$, 191.4 Hz⁴¹ and its variation with the exchange and correlation functionals are 17 and 4 Hz, respectively. Regarding the effects of the exchange functionals on this contribution, we can distinguish a small group consisting of OPTX, BRx, PKZB, and TPSS that yields the smallest contributions in magnitude. Thus, when the contribution is negative (5 out of 16 represented values) these functionals yield the largest PSO values. It should be noted that exchange and correlation functional effects are independent of each other. Using the cheap local Slater functional, the PSO MCSCF contributions can be reproduced with rmsd/mad of 0.76/0.34 r.u. (0.96/0.44 Hz). Deviations from these MCSCF results higher than 1 Hz correspond to fluorine involved SSCCs: ${}^1J_{HF}^{PSO}$ (HF molecule), ${}^2J_{HF}^{PSO}(\text{CH}_3\text{F})$, and ${}^1J_{CF}^{PSO}(\text{CH}_3\text{F})$ that amount to 4.8, 2.8, and 2.0 Hz, respectively.

As an example, only the results of four DSO contributions are depicted in the Supporting Information. The values for this contribution lie between -2 and 7 Hz, and often, specially when they are larger, the PSO and the DSO contributions cancel each other. Besides, although its magnitude may not seem negligible, its variation with the type of exchange or correlation functional is very small. The maximum variation is 0.1 Hz in ${}^1K_{HF}^{DSO}(\text{HF})$. Owing to their small values, these maximum variations are not included in Table 1. DSO contributions can be calculated with any XC functional, because their uncertainty is much lower than that included in the remaining contributions.

After the above analysis, we focus our attention on the FC contribution. Taking MCSCF calculated values⁴¹ as reference, we note that the behavior of FC contributions calculated with Slater and those calculated at the HF are opposite to each other in most SSCCs. In Figure 2, the relative deviations $[J^{FC}(\text{Slater or HF}) - J^{FC}(\text{MCSCF})]/J^{FC}(\text{MCSCF})$ for the calculated FC contribution are represented. Notice that owing to the larger deviations obtained with the HF method, they have been represented using a large scale (upper scale). Out of range values are indicated numerically and the SSCCs where the MCSCF results do not fall between those of Slater and HF are shown with an asterisk. Only six results correspond to this group, three are geminal and three are vicinal couplings. This leads us to consider that using the combination of a fraction $(1 - a_x)$ of Slater exchange functional and a fraction a_x of exact HF, the behavior of the MCSCF results could be approximated reasonably.

4. EFFECT OF THE HF EXCHANGE

The HF exchange effect on the SSCCs can be studied using the following general expression

$$E_{XC}^{\text{hybrid}} = a_x E_x^{\text{HF}} + (1 - a_x) E_x^S + E_c \quad (13)$$

where E_x^{HF} represents the HF exchange contribution, E_x^S is the Slater exchange functional and E_c is the correlation functional. The adjustable parameter a_x is the fraction of HF exchange included in the calculation.

Total RSSCCs and their respective four contributions have been calculated for the indicated molecules using different percentages of HF exchange. These percentages have been changed from 0 to 100% at intervals of 10%. Figure 3 shows some representative results for ${}^1K_{NM}$ and ${}^2K_{NM}$ RSSCCs. We can see that the behavior of the calculated values for these RSSCCs as a function of the HF exchange percentage is not homogeneous. There are values that increase with the HF exchange portion, while others decrease. It is also noted a large variation in the RSSCCs when the HF exchange percentage is higher than 70–80%. This variation, which can be attributed to the well-known triplet-instability problem,^{4,28} is higher when the correlation energy, that is, the correlation functional, is not considered.

All ${}^1K_{NM}$ values studied here, without exception, increase with the HF exchange fraction. That does not happen to ${}^1J_{NM}$ because some couplings in frequency units change their sign relative to reduced units. This makes ${}^1J_{OH}$, ${}^1J_{CO}$, ${}^1J_{CN}$ and ${}^1J_{NN}$ decrease as the percentage of HF exchange considered increases.

Geminal and vicinal RSSCCs, due to their lower magnitude, tend to be less sensitive to the used exact exchange fraction. Nevertheless, we found two opposing trends. Thus, ${}^2K_{CH}$, ${}^2K_{HH}$, and ${}^2K_{NH}$ decrease as the HF exchange increases, while ${}^2K_{FH}$ and ${}^2K_{OO}$ increase. The only coupling that changes its sign, when passing to Hz, is that of ${}^2K_{NH}$ in HCN, so ${}^2J_{NH}$ has opposite behavior to that of ${}^2K_{NH}$.

An interesting fact is that most of the results that include correlation functional, cross the experimental value when moving from considering the Slater potential to the HF one. Results shown in Figure 3 corroborate the parallel behavior exhibited by the results of correlation energy functionals discussed here and the great variation produced in some RSSCCs when the Slater local exchange is either not considered or considered in a small percentage.

Because the values of these RSSCCs are obtained, according to the Ramsey nonrelativistic theory, as the sum of four contributions (FC, SD, PSO, and DSO), it is worth analyzing the sensitivity of these components with respect to the fraction of HF exchange. It would be interesting to examine in detail the different behavior of these contributions, but is beyond the scope of this work. We will just expose their general behavior in order to consider the possible use of a functional with optimum percentage of exact exchange to obtain results with acceptable accuracy.

First, it is well-known that not all components contribute in the same proportion and that this proportion depends on the type of RSSCCs (vide supra). Figure 4 shows the behavior of the four Ramsey contributions for some representative RSSCCs. Although Figure 4 shows only the results for one ${}^1K_{CC}$ that of C_2H_4 , its behavior is analogous to all ${}^1K_{CC}$ for all remaining analyzed compounds, and also to that of ${}^1K_{XH}$ (remember the change of sign for ${}^1J_{OH}$ in H_2O). In all of them, the FC contribution is the most important, whereas the other terms are small and show little sensitivity to the used HF exchange portion. The same applies to the ${}^1K_{CF}$ constant.

For ${}^1K_{FH}$ in hydrogen fluoride, the FC contribution behaves similarly to the other ${}^1K_{NM}$ RSSCCs, but the PSO contribution becomes very relevant. However, PSO values, as in the other RSSCCs, remain constant with the used HF exchange potential. ${}^1K_{CO}$ presents a similar behavior to that of ${}^1K_{OH}$ in H_2O .

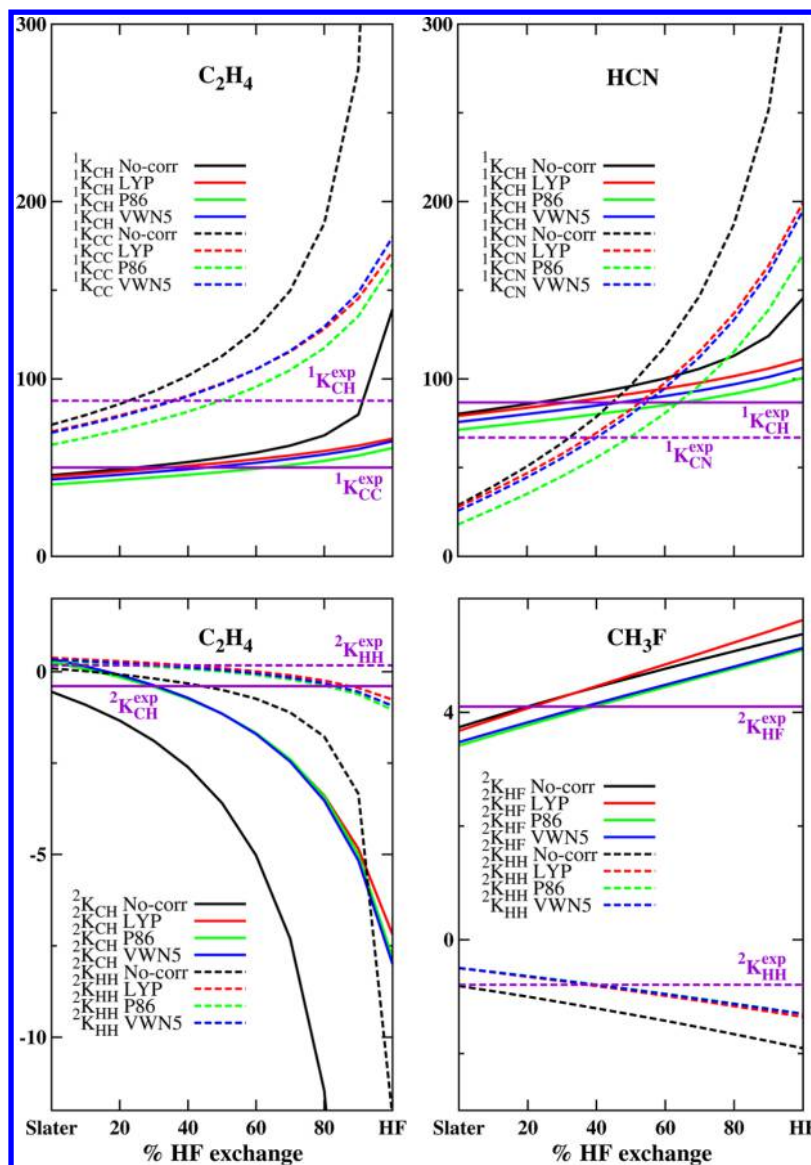


Figure 3. Variation in $^1K_{NM}$ and $^2K_{NM}$ vs the percentage of HF exchange included for some representative molecules.

Its $^1J_{CO}^{FC}$ contribution decreases with the percentage of HF exchange. In these couplings, the PSO term is not negligible, although is not very sensitive to the used exchange portion. $^1K_{NN}$ (N_2) and $^1K_{CN}$ (HCN) have significant SD and PSO contributions compared to the FC term. Again, they have a small variation versus the exact exchange potential percentage than that of FC.

Figure 4 shows also the calculated contributions for some geminal RSSCCs. These plots are representative of the analogous RSSCCs studied in this work for several compounds. For geminal RSSCCs the SD contribution is small and PSO and DSO compensate each other, resulting in a small non contact contribution. Exceptions are $^2K_{OO}$ (CO_2) and $^2K_{FH}$ (CH_3F). It should be noted that the non contact contribution is not negligible since FC one is small. For $^2K_{FH}$ the situation is different because both PSO and FC are relevant. Regarding $^2K_{OO}$ (CO_2), Figure 4 shows that SD and PSO contributions become important. They present small variation on the used HF exchange and their sign is opposite to that of FC one, which is very sensitive to the type of exchange. The DSO contribution is negligible. Although $^2K_{NH}$ RSSCC is not shown, its behavior is

similar to that of $^2K_{CH}$, with a PSO value similar to the FC one, while the SD and DSO contributions are smaller.

Summing up, the FC contribution is much more sensitive to the type of exchange used than the rest of the components, except in the N_2 molecule, where the SD and PSO contributions show considerable variation with the type of exchange. The DSO component is invariant with respect to the exchange potential. SD and PSO components, in general, are not sensitive to the exact exchange used, although their values are very important in SSCCs where a fluorine nucleus is involved.

5. EXACT EXCHANGE FITTINGS AND HYBRID EXCHANGE FUNCTIONALS

The dependence of each type of SSCC on the fraction of HF exchange a_w , eq 13, was obtained by fitting each set of calculated SSCCs i to a polynomial,

$$J_i^{fitted}(a_x) = J_{i0} + J_{i1} \cdot a_x + J_{i2} \cdot (a_x)^2 + J_{i3} \cdot (a_x)^3 + \dots \quad (14)$$

where $J_{i,n}$ with $n = 0, 1, \dots$ are the fitted coefficients for the corresponding set i of SSCCs calculated with a particular

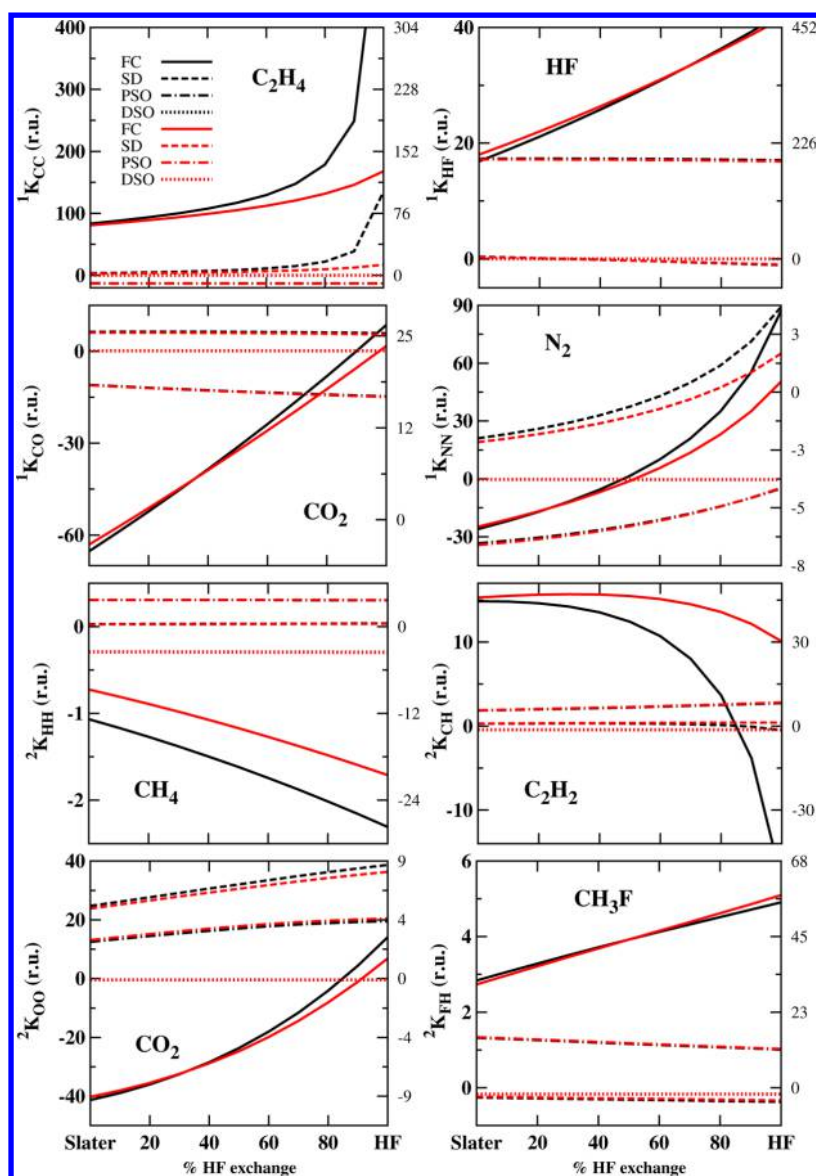


Figure 4. Variation in ${}^nK_{NMP}^{FC}$, ${}^nK_{NMP}^{SD}$, ${}^nK_{NMP}^{PSO}$, and ${}^nK_{NMP}^{DSO}$ contributions vs the percentage of HF exchange included for some representative contributions and molecules. Slater (black curves) and Slater plus LYP (red curves) functionals are shown. Right-hand axis corresponds to the contribution in Hz.

functional. In order to avoid problems with triplet instabilities or quasi-instabilities^{4,28} when large percentage of HF exchange is included, only values between 0 and 80% of exact exchange are considered in the fits. Four functionals have been studied, Slater/HF and Slater/HF plus LYP, VWN5, and P86 correlation functionals.

For the whole set of SSCCs and for each type of functional, three statistical parameters are minimized over a_x :

$$\text{rmsd} - J = \sqrt{\frac{\sum_i (J^{\text{exp}} - J_i^{\text{fitted}}(a_x))^2}{n - 1}} \quad (15)$$

$$\text{rmsd} - K = \sqrt{\frac{\sum_i (K^{\text{exp}} - K_i^{\text{fitted}}(a_x))^2}{n - 1}} \quad (16)$$

$$\text{rmsd} - R = \sqrt{\frac{\sum_i ((J^{\text{exp}} - J_i^{\text{fitted}}(a_x))/J^{\text{exp}})^2}{n - 1}} \quad (17)$$

where n is the number of calculated/experimental SSCCs, which, in this work, is 39. The first two statistics correspond to root-mean-square deviation using J SSCCs in frequency units (Hz) and RSSCCs in reduced units, respectively.⁴¹ The third parameter is a relative root-mean-square deviation.

The choice of the statistical parameter is rather relevant because the optimized a_x value depends on it. The use of a different parameter is similar to the use of a different weight for each SSCC. From an experimental point of view, the percentage of HF exchange obtained using the rmsd-J will predict better SSCCs in Hz. However, in a multinuclear study and from a theoretical point of view, the use of RSSCCs should be better since they only depend on the electronic coupling mechanism and do not depend on the nuclear gyromagnetic ratios. The statistic rmsd-R appears to be informative when SSCCs exhibit different magnitudes. However, when the SSCCs are close to zero, the relative deviations can be large, causing a distortion in the rmsd-R results. Besides the three statistical parameters used in the minimization, the mean absolute deviations (mads) have been calculated for the minima in the three cases (mad-J, mad-K and mad-R).

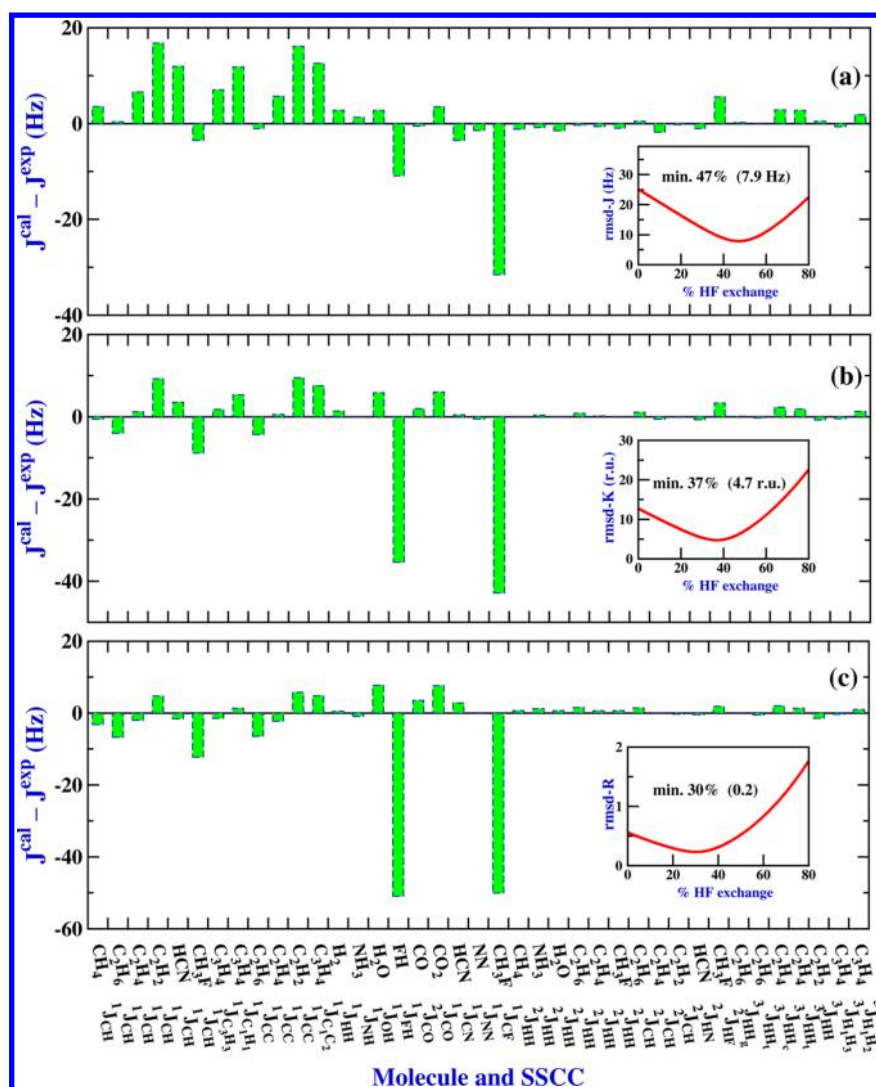


Figure 5. Deviations calculated with Slater in combination with the HF exchange plus LYP correlation functional corresponding to the minimum of (a) rmsd-J, (b) rmsd-K, and (c) rmsd-R, whose variations are represented in the inset figures.

Deviations from the experimental values $J^{\text{cal}} - J^{\text{exp}}$, in Hz, corresponding to the minimum are presented in Figure 5. The results of this figure are those obtained with the Slater in combination with the corresponding fraction of exact exchange plus LYP correlation functional. Representations for other XC functionals are qualitatively similar. The variation of the three statistical parameters (rmsd-J, rmsd-K, and rmsd-R) against the included fraction of exact exchange is represented in the insets of Figure 5. The three curves present a minimum lying between 30 and 47% of the HF exchange (see Table 2). When the rmsd-K or rmsd-R statistical parameters are used in the minimization, two values deviate significantly: that of $^1J_{\text{FH}}$ in hydrogen fluoride (deviate -35 and -51 Hz, respectively) and $^1J_{\text{CF}}$ in CH_3F (-43 and -50 Hz). This last SSCC deviates also appreciably (-32 Hz) when the rmsd-J is used in the minimization. Results obtained when these two SSCCs are not considered are shown in Table S2. Moreover, when the minimization criterion is that of rmsd-J, important deviations for $^1J_{\text{CH}}$ and $^1J_{\text{CC}}$ in C_2H_2 appear that deviate 17 and 16 Hz, respectively.

For comparison, the statistical parameters have been applied to SSCCs obtained with other wave function and density functional methods. These results are presented in Table 2. Although the best results are those of the MCSCF⁴¹ and SOPPA(CCSD),

Table 2. Statistical Results for the Set of Studied SSCCs

method	rmsd-J/mad-J (Hz)	rmsd-K/mad-K (r.u.)	rmsd-R/mad-R
MCSCF	3.49/2.08	2.53/1.19	0.26/0.12
SOPPA(CCSD)	3.71/2.66	4.96/2.36	0.41/0.20
SOPPA	6.55/4.62	6.63/3.47	0.59/0.29
PBE	30.02/9.86	12.01/5.68	0.39/0.24
B3LYP	20.70/10.05	8.66/4.84	0.29/0.18
B3PW91	23.72/8.46	8.88/4.48	0.33/0.20
B3P86	23.80/8.18	8.87/4.40	0.30/0.17
B97-2	16.32/6.19	7.12/3.37	0.22/0.13
Smm ^a	11.89/7.67 (41%)	6.10/3.21 (30%)	0.40/0.24 (0%)
SmmLYP ^a	7.88/4.60 (47%)	4.74/2.39 (37%)	0.23/0.13 (30%)
SmmVWN5 ^a	7.33/4.54 (55%)	5.09/2.72 (39%)	0.21/0.13 (32%)
SmmP86 ^a	6.51/4.45 (66%)	4.83/2.91 (51%)	0.28/0.19 (33%)

^aFigures in parentheses are the HF exchange percentage (mm) included in the calculation.

the calculated DFT values using a fitted fraction of exact exchange improve significantly over the remaining DFT results. Thus, when S47LYP is used the rmsd-J/mad-J is 7.9/4.6 Hz, while those obtained with MCSCF, SOPPA(CCSD) and SOPPA are 3.5/2.1,

3.7/2.7, and 6.6/4.6 Hz, respectively, and those corresponding to standard functionals lie between 16.3/6.2 and 30.0/9.9 Hz. Considering rmsd-K in the minimization, DFT results (between 4.7 and 6.1 r.u.) are statistically similarly to those of both SOPPA methods (between 5.0 and 6.6 r.u.). When rmsd-R is used, this statistical parameter calculated including correlation functional is between 0.21 and 0.28, while the MCSCF result yields 0.26. It should be noted that results improve even without the correlation functional over the standard functionals; however, the three statistics are worse than those obtained when the correlation functional is considered.

The four optimized hybrid functionals shown in Table 2 and in Table S2 have been tested on a set of $^1J_{CH}$ SSCCs that has been recently studied in detail.¹⁵ This data set is formed by 88 carbon–proton SSCCs. The coupled carbon presents hybridization of sp^3 , sp^2 , sp , or aromatic types. To compare experimental and calculated values, rovibrational contributions of 5 Hz were subtracted from the former ones to obtain the so-called empirical values. This rough estimation of that rovibrational contributions has been justified previously.^{15,20} For this assessment, S66P86 functional yields rmsd/mad of 4.2/3.0 Hz, which is similar to the best ones obtained previously.¹⁵ The best results were those obtained¹⁵ with the functional B3P86 when the geometry is optimized at the same level of theory. There, the rmsd/mad value was 4.3/2.8 Hz (see Table 2 in ref 15). The statistical results (rmsd/mad) obtained with S41, S47LYP, and S5SVWN5 are 10.8/8.8, 7.6/6.1, and 5.7/4.4 Hz, respectively. The percentage of HF exchange included in these calculations were not optimized exclusively for $^1J_{CH}$ SSCCs, although 8 out of 39 experimental SSCCs correspond to this type. To get better quantitative results, an alternative procedure could be the optimization of that percentage for each type of SSCC. For instance, the application of S24 instead of S41 to this data set, percentage obtained when the couplings involving fluorine are ignored (see Supporting Information), improves the rmsd/mad of this economical functional from 11.9/7.7 to 5.2/4.2 Hz.

It should be pointed out that the 39 experimental SSCCs have been used in this work to analyze the functional behavior. Therefore, the optimized functionals presented in Table 2 are tentative, as they will depend on the data set used. For instance, in this case results could be biased toward 1K RSSCCs. In Table 3,

Table 3. Statistical rmsd-K/mad-K (r.u.) for Three Subsets (1K , 2K , and 3K)^a of RSSCCs

method	1K	2K	3K
MCSCF	3.48/2.13	0.14/0.10	0.09/0.07
SOPPA(CCSD)	6.83/4.22	0.34/0.24	0.11/0.09
SOPPA	9.13/6.24	0.41/0.33	0.15/0.12
SmmP86 ^b	6.64/5.22 (51%)	0.32/0.21 (35%)	0.10/0.08 (37%)

^aSubsets: 1K , 2K , and 3K correspond to one bond, geminal and vicinal nK RSSCCs, respectively. ^bFigures in parentheses are the HF exchange percentage (mm) included in the calculation.

results obtained for one-bond 1K , geminal 2K , and vicinal 3K RSSCCs are shown for MCSCF, SOPPA(CCSD), SOPPA, and SmmP86 functional. For the subset 1K containing 21 values (out of 39 experimental), we observe that rmsd-K/mad-K are larger than those corresponding to the full set (see the rmsd-K/mad-K column in Table 2), while its optimized percentage of HF exchange is the same (51%). Clearly, set 1K has larger values than sets 2K and 3K . For this reason, statistics worsen for 1K and improve for 2K and 3K . The optimized percentage of HF exchange

decreases to 35% and 37%, respectively, for 2K and 3K . However, maintaining a percentage of 51% the statistical results for 2K and 3K are close to those of Table 3, due to small numerical values presented for these types of SSCCs. We show that a combination of local and nonlocal exchange improves DFT methods near to the more expensive SOPPA method.

SSCCs calculations using DFT are less demanding regarding the basis set size than wave functions methods as multireference ones, and it has been shown⁶³ that a triple- ζ basis set almost reaches convergence to experimental SSCCs. In this work, we use the aug-cc-pVTZ-J,²⁸ which is a medium-large basis set (126 basis functions for methane) that has proved to give results similar to those obtained with larger basis sets. For instance, for $^1J_{CH}$ the results using aug-cc-pVTZ-J are similar to those obtained with the pcJ-3⁶⁵ (269 basis functions for methane) and ccJ-pVQZ⁶⁴ (227 basis functions for methane), see Table 1 and Figure 3 in ref 15. Despite these previous results, we have tested the performance of the functionals developed in this work using those large basis sets to predict the experimental set of 39 SSCCs. It should be noted that these basis set were also specially built to calculate SSCCs. The results are presented in Table S3, and comparison with those of Table 2 shows that there is no qualitative difference between these results and those obtained with the aug-cc-pVTZ-J. Thus, when the S66P86 functional is used with the pcJ-3 and ccJ-pVQZ basis sets, the rmsd-J/mad-J are 6.0/4.0 and 6.1/4.2 Hz, respectively, while those obtained with the smaller aug-cc-pVTZ basis set are 6.5/4.5 Hz.

6. CONCLUDING REMARKS

The performance of more than 130 density functionals were tested for their ability to predict 45 diverse SSCCs in 14 molecules. This SSCC set includes one-, two- and three-bond SSCCs transmitted through single, double and triple bonds, and coupled atoms of varied electronegativity with and without lone pair. A large number of exchange and correlation functionals has been combined to obtain the main trends on total SSCCs as well as on their four Ramsey contributions.

Effects of exchange and correlation functionals upon SSCCs are rather independent, allowing the combination no matter their origin and with no artifacts. Considering the FC contributions, results for BRx, OPTX, TPSS, and in lesser amount G96 exchange functionals deviate appreciably from the average results of all the others. With few exceptions, the BRx exchange functional increases the magnitude of the RSSCCs significantly. The correlation functionals decrease one- and three-bond RSSCCs, while they increase two-bond RSSCCs. Taking into account that the geminal RSSCCs are, in general, negative, the correlation functional increases the magnitude of FC reduced contributions. SD and PSO contributions present, in general, smaller values and variations with the exchange or correlation functional than the FC ones. DSO component is insensitive to the used exchange and correlation functionals and is even less sensitive to the percentage of HF exchange considered. Therefore, the non contact contributions could be calculated reasonably using the efficient local Slater functional.

The dependence of the SSCCs on the fraction of the HF exchange can be represented by a polynomial. In this work, this variation is reproduced using a cubic polynomial. However, similar results are obtained using a second order equation. Considering this dependence, an optimization of fraction of the HF exchange part has been carried out. In this work, accurate SSCCs are obtained using the local Slater exchange functional in

combination with a percentage of the HF exchange and including correlation functionals, namely, LYP, VWN5, or P86.

Thus, the S47LYP functional predicts the experimental SSCCs of our data set with rmsd/mad of 7.9/4.6 Hz, which is worse than the values obtained with multideterminantal wave function methods as MCSCF and SOPPA(CCSD), but similar to those obtained with SOPPA, and better than those obtained with common DFT functionals. Considering reduced SSCCs, the S51P86 functional yields rmsd-K/mad-K values (4.8/2.9 r.u) that are close to and better than those of SOPPA(CCSD) and SOPPA, respectively. In general, the use of this kind of purpose functional (local X + nonlocal X + correlation) improves calculated SSCC values with a cheap computational cost. For example, we have applied the particular S66P86 functional to a data set of 88 $^1J_{CH}$ SSCCs¹⁵ obtaining one of the best results with rmsd/mad of 4.2/3.0 Hz.

Finally, we will remark that SSCCs between nuclei with lone pair and, specially, when a fluorine is involved in the coupling are difficult to calculate using DFT methods. They present the largest deviations from the experimental values as well as contradictory behavior within the calculated results. This is a well-known drawback of the DFT methods, that is, "fluorine problem".⁶⁶ Therefore, it is a challenge for future functional developments.

■ ASSOCIATED CONTENT

● Supporting Information

Representations for the calculated FC, SD, PSO and DSO contributions using different exchange and correlation functionals; deviations calculated with Slater, HF exchange and LYP correlation functional for the minimum of rmsd-J, rmsd-K and rmsd-R, excluding $^1J_{HF}$ and $^1J_{CF}$ in HF and CH_3F SSCCs; and maximum exchange functional variations (MXFV) and maximum correlation functional variations (MCFV) of couplings (Hz) for FC, SD, and PSO contributions. This material is available free of charge via the Internet at <http://pubs.acs.org>.

■ AUTHOR INFORMATION

Corresponding Author

*E-mail: garcia.delavega@uam.es.

Funding

The following financial support is gratefully acknowledged: Ministerio de Ciencia e Innovación (MICINN) project no. FIS2012-35880, the Universidad de Alicante and Spanish Agency of International Co-operation, project no. A1/035856/11. Computer time provided by the Centro de Computación Científica de Universidad Autónoma de Madrid is gratefully acknowledged.

Notes

The authors declare no competing financial interest.

■ DEDICATION

This work is dedicated to the memory of Prof. Ruben H. Contreras, who kept enthusiasm and passion for science until the last moment.

■ REFERENCES

- (1) Becke, A. D. *J. Chem. Phys.* **2014**, *140*, 18A301.
- (2) Malkin, V. G.; Malkina, O. L.; Salahub, D. R. *Chem. Phys. Lett.* **1994**, *221*, 91.
- (3) Krivdin, L. B.; Contreras, R. H. *Annu. Rep. NMR Spectrosc.* **2007**, *61*, 133.

- (4) Helgaker, T.; Jaszunski, M.; Pecul, M. *Prog. Nucl. Magn. Reson. Spectrosc.* **2008**, *53*, 249.
- (5) Suardiaz, R.; Pérez, C.; Crespo-Otero, R.; García de la Vega, J. M.; San Fabián, J. *J. Chem. Theory Comput.* **2008**, *4*, 448.
- (6) Bartlett, R. J.; Sekino, H. In *Nonlinear Optical Materials: Theory and Modeling*; Karna, S. P., Yeates, A. T., Eds.; ACS Symposium Series; American Chemical Society: Washington, DC, 1996; Vol. 628; p 23.
- (7) Becke, A. D. *J. Chem. Phys.* **1993**, *98*, 5648.
- (8) Lee, C.; Yang, W.; Parr, R. G. *Phys. Rev. B* **1988**, *37*, 785.
- (9) Sychrovský, V.; Gräfenstein, J.; Cremer, D. *J. Chem. Phys.* **2000**, *113*, 3530.
- (10) Helgaker, T.; Watson, M.; Handy, N. C. *J. Chem. Phys.* **2000**, *113*, 9402.
- (11) Lantto, P.; Vaara, J.; Helgaker, T. *J. Chem. Phys.* **2002**, *117*, 5998.
- (12) Kupka, T. *Chem. Phys. Lett.* **2008**, *461*, 33.
- (13) Kupka, T. *Magn. Reson. Chem.* **2009**, *47*, 674.
- (14) Nazarsky, R. B.; Makulski, W. *Phys. Chem. Chem. Phys.* **2014**, *16*, 15699.
- (15) San Fabián, J.; García de la Vega, J. M.; Fernández-Oliva, M.; Pérez, C.; Crespo-Otero, R.; Contreras, R. H. *Magn. Reson. Chem.* **2013**, *51*, 775.
- (16) Schäfer, A.; Horn, H.; Ahlrichs, R. *J. Chem. Phys.* **1992**, *97*, 2571.
- (17) Schütz, M.; Brdarski, S.; Widmark, P.-O.; Lindh, R.; Karlstrom, G. *J. Chem. Phys.* **1997**, *107*, 4597.
- (18) Perdew, J. P.; Burke, K.; Ernzerhof, M. *Phys. Rev. Lett.* **1996**, *77*, 3865.
- (19) Perdew, J. P.; Burke, K.; Ernzerhof, M. *Phys. Rev. Lett.* **1997**, *78*, 1396.
- (20) Maximoff, S. N.; Peralta, J. E.; Barone, V.; Scuseria, G. E. *J. Chem. Theory Comput.* **2005**, *1*, 541.
- (21) Cunha Neto, A.; dos Santos, F. P.; Paula, A. S.; Tormena, C. F.; Rittner, R. *Chem. Phys. Lett.* **2008**, *454*, 129.
- (22) Perdew, J. P. In *Electronic Structure of Solids '91*; Ziesche, P., Eschrig, H., Eds.; Akademie Verlag: Berlin, 1991; p 11.
- (23) Perdew, J. P.; Chevary, J. A.; Vosko, S. H.; Jackson, K. A.; Peterson, M. R.; Singh, D. J.; Fiolhais, C. *Phys. Rev. B* **1992**, *46*, 6671.
- (24) Perdew, J. P.; Chevary, J. A.; Vosko, S. H.; Jackson, K. A.; Peterson, M. R.; Singh, D. J.; Fiolhais, C. *Phys. Rev. B* **1993**, *48*, 4978.
- (25) Perdew, J. P. *Phys. Rev. B* **1986**, *33*, 8822.
- (26) Wilson, P. J.; Bradley, T. J.; Tozer, D. J. *J. Chem. Phys.* **2001**, *115*, 9233.
- (27) Keal, T. W.; Helgaker, T.; Salek, P.; Tozer, D. J. *Chem. Phys. Lett.* **2006**, *425*, 163.
- (28) Provasi, P. F.; Aucar, G. A.; Sauer, S. P. A. *J. Chem. Phys.* **2001**, *115*, 1324.
- (29) Kupka, T.; Nieradka, M.; Stachów, M.; Pluta, T.; Nowak, P.; Kjær, H.; Kongsted, J.; Kaminsky, J. *J. Phys. Chem. A* **2012**, *116*, 3728.
- (30) Becke, A. D. *J. Chem. Phys.* **1993**, *98*, 1372.
- (31) Perdew, J. P.; Ernzerhof, M.; Burke, K. *J. Chem. Phys.* **1996**, *105*, 9982.
- (32) Tozer, D. J. *J. Chem. Phys.* **2000**, *112*, 3507.
- (33) Rohrdanz, M. A.; Martins, K. M.; Herbert, J. M. *J. Chem. Phys.* **2009**, *130*, 054112.
- (34) Morrell, M. M.; Parr, R. G.; Levy, M. J. *J. Chem. Phys.* **1975**, *62*, 549.
- (35) Engel, E.; Chevary, J.; Macdonald, L.; Vosko, S. Z. *Phys. D: At., Mol. Clusters* **1992**, *23*, 7.
- (36) Jaramillo, J.; Scuseria, G. E.; Ernzerhof, M. *J. Chem. Phys.* **2003**, *118*, 1068.
- (37) Arbuznikov, A. V.; Bahmann, H.; Kaupp, M. *J. Phys. Chem. A* **2009**, *113*, 11898.
- (38) Arbuznikov, A. V.; Kaupp, M. *Int. J. Quantum Chem.* **2011**, *111*, 2625.
- (39) Dirac, P. A. M. *Proc. Cambridge Philos. Soc.* **1930**, *26*, 376.
- (40) Slater, J. C. *Phys. Rev.* **1951**, *81*, 385.
- (41) San Fabián, J.; Díez, E.; Giarca de la Vega, J. M.; Suardiaz, R. *J. Chem. Phys.* **2008**, *128*, 084108.
- (42) Becke, A. D. *Phys. Rev. A* **1988**, *38*, 3098.
- (43) Adamo, C.; Barone, V. *J. Chem. Phys.* **1999**, *110*, 6158.
- (44) Gill, P. M. W. *Mol. Phys.* **1996**, *89*, 433.

- (45) Adamo, C.; Barone, V. *J. Chem. Phys.* **1998**, *108*, 664.
- (46) Ernzerhof, M.; Perdew, J. P. *J. Chem. Phys.* **1998**, *109*, 3313.
- (47) Handy, N. C.; Cohen, A. J. *Mol. Phys.* **2001**, *99*, 403.
- (48) Hoe, W.-M.; Handy, N. C.; Cohen, A. J. *Chem. Phys. Lett.* **2001**, *341*, 319.
- (49) Becke, A. D.; Roussel, M. R. *Phys. Rev. A* **1989**, *39*, 3761.
- (50) Perdew, J. P.; Kurth, S.; Zupan, A.; Blaha, P. *Phys. Rev. Lett.* **1999**, *82*, 2544.
- (51) Tao, J.; Perdew, J. P.; Staroverov, V. N.; Scuseria, G. E. *Phys. Rev. Lett.* **2003**, *91*, 146401.
- (52) Vosko, S. H.; Wilk, L.; Nusair, M. *Can. J. Phys.* **1980**, *58*, 1200.
- (53) Perdew, J. P.; Zunger, A. *Phys. Rev. B* **1981**, *23*, 5048.
- (54) Frisch, M. J.; Trucks, G. W.; Schlegel, H. B.; Scuseria, G. E.; Robb, M. A.; Cheeseman, J. R.; Scalmani, G.; Barone, V.; Mennucci, B.; Petersson, G. A.; Nakatsuji, H.; Caricato, M.; Li, X.; Hratchian, H. P.; Izmaylov, A. F.; Bloino, J.; Zheng, G.; Sonnenberg, J. L.; Hada, M.; Ehara, M.; Toyota, K.; Fukuda, R.; Hasegawa, J.; Ishida, M.; Nakajima, T.; Honda, Y.; Kitao, O.; Nakai, H.; Vreven, T.; Montgomery, J. A., Jr.; Peralta, J. E.; Ogliaro, F.; Bearpark, M.; Heyd, J. J.; Brothers, E.; Kudin, K. N.; Staroverov, V. N.; Kobayashi, R.; Normand, J.; Raghavachari, K.; Rendell, A.; Burant, J. C.; Iyengar, S. S.; Tomasi, J.; Cossi, M.; Rega, N.; Millam, J. M.; Klene, M.; Knox, J. E.; Cross, J. B.; Bakken, V.; Adamo, C.; Jaramillo, J.; Gomperts, R.; Stratmann, R. E.; Yazyev, O.; Austin, A. J.; Cammi, R.; Pomelli, C.; Ochterski, J. W.; Martin, R. L.; Morokuma, K.; Zakrzewski, V. G.; Voth, G. A.; Salvador, P.; Dannenberg, J. J.; Dapprich, S.; Daniels, A. D.; Farkas, A. C.; Foresman, J. B.; Ortiz, J. V.; Cioslowski, J.; Fox, D. J. *Gaussian 09*, revision B01, Gaussian, Inc.: Wallingford, CT, 2010.
- (55) Becke, A. D. *J. Chem. Phys.* **1996**, *104*, 1040.
- (56) Rey, J.; Savin, A. *Int. J. Quantum Chem.* **1998**, *69*, 581.
- (57) Krieger, J. B.; Chen, J. Q.; Iafrate, G. J.; Savin, A. In *Electron Correlations and Materials Properties*; Gonis, A., Kioussis, N., Ciftan, M., Eds.; Kluwer Academic: New York, 1999; p 463.
- (58) Toulouse, J.; Savin, A.; Adamo, C. *J. Chem. Phys.* **2002**, *117*, 10465.
- (59) Slater, J. *The Self-Consistent Field for Molecular and Solids, Quantum Theory of Molecular and Solids*; McGraw-Hill: New York, 1974.
- (60) Nielsen, E. S.; Jorgensen, P.; Oddershede, J. *J. Chem. Phys.* **1980**, *73*, 6238.
- (61) Sauer, S. P. A. *J. Phys. B: At. Mol. Opt. Phys.* **1997**, *30*, 3773.
- (62) Enevoldsen, T.; Oddershede, J.; Sauer, S. P. A. *Theor. Chem. Acc.* **1998**, *100*, 275.
- (63) Peralta, J. E.; Scuseria, G. E.; Cheeseman, J. R.; Frisch, M. J. *Chem. Phys. Lett.* **2003**, *375*, 452.
- (64) Benedikt, U.; Auer, A. A.; Jensen, F. *J. Chem. Phys.* **2008**, *129*, 064111.
- (65) Jensen, F. *J. Chem. Theory Comput.* **2006**, *2*, 1360.
- (66) Vaara, J. *Phys. Chem. Chem. Phys.* **2007**, *9*, 5399.